Deficiency of filamin A in smooth muscle cells protects against hypoxia-mediated pulmonary hypertension in mice

YAGUO ZHENG[1*], HONG MA[2*], YUFENG YAN[1], PENG YE[1], WANDE YU[1], SONG LIN[1] and SHAO-LIANG CHEN[1]

[1]Department of Cardiology, Nanjing First Hospital, Nanjing Medical University, Nanjing, Jiangsu 210008;
[2]Department of Cardiology, First Affiliated Hospital of Nanjing Medical University, Nanjing, Jiangsu 210029, P.R. China

Abstract. Filamin A (FLNA) is a high molecular weight cytoskeleton protein important for cell locomotion. A relationship between FLNA mutations and pulmonary arterial hypertension (PAH) has previously been reported; however, the detailed mechanism remains unclear. The present study aimed to explore the role of FLNA in vascular smooth muscle cells during the development of PAH. Smooth muscle cell (SMC)-specific FLNA-deficient mice were generated and the mice were then exposed to hypoxia for 28 days to build the mouse model of PAH. Human pulmonary arterial smooth muscle cells (PASMCs) were also cultured and transfected with FLNA small interfering RNA or overexpression plasmids to investigate the effects of FLNA on PASMC proliferation and migration. Notably, compared with control individuals, the expression levels of FLNA were increased in lung tissues from patients with PAH, and it was obviously expressed in the PASMCs of pulmonary arterioles. FLNA deficiency in SMCs attenuated hypoxia-induced pulmonary hypertension and pulmonary vascular remodeling. *In vitro* studies suggested that absence of FLNA impaired PASMC proliferation and migration, and produced lower levels of phosphorylated (p)-PAK-1 and RAC1 activity. However, FLNA overexpression promoted PASMC proliferation and migration, and increased the expression levels of p-PAK-1 and RAC1 activity. The present study highlights the role of FLNA in pulmonary vascular remodeling; therefore, it could serve as a potential target for the treatment of PAH.

Correspondence to: Dr Song Lin or Dr Shao-Liang Chen, Department of Cardiology, Nanjing First Hospital, Nanjing Medical University, 68 Changle Road, Qinhuai, Nanjing, Jiangsu 210008, P.R. China
E-mail: linsong19711991@sina.com
E-mail: chmengx1964@126.com

*Contributed equally

Introduction

Pulmonary arterial hypertension (PAH) is a devastating disease characterized by increased pulmonary vascular resistance and right heart dysfunction, eventually leading to right heart failure and premature death (1). Although several molecular signaling pathways have been demonstrated to participate in pulmonary vascular remodeling, the underlying mechanisms are still unclear (2,3). Current targeted therapies can relieve clinical symptoms, but disease progression is inevitable in the majority of patients and the prognosis is still poor (4). Therefore, it is necessary to explore novel mechanisms and search for more efficacious therapies in this area.

Filamin A (FLNA) is a high molecular weight cytoskeleton protein encoded by the X-linked gene FLNA. It is mainly located in the cytoplasm as a V-shaped homodimer (5). As a scaffold protein, FLNA not only stabilizes cytoskeleton structure, but also serves an important role in signal transduction. FLNA gene mutations can cause periventricular nodular heterotopia, which is an X-linked dominant genetic disease in which neurons fail to migrate to the cerebral cortex (5). As well as neurological manifestations, other abnormalities, particularly cardiovascular symptoms, are also common in patients with FLNA mutations (6). Previous studies have revealed that FLNA mutations may also be associated with lung diseases, especially pulmonary hypertension. Eltahir *et al* (7) reported a case of FLNA gene mutation, which manifested as acute respiratory distress and pulmonary hypertension. Burrage *et al* (8) described a cohort of six infants with a pathogenic variant in the FLNA gene; all of the patients presented with pulmonary hypertension and progressive respiratory failure, and received lung transplantation as a viable therapeutic option. Hirashiki *et al* (9) also reported two cases of FLNA gene mutation in inherited pulmonary hypertension. These studies suggested that FLNA may be associated with pulmonary hypertension; however, the exact mechanism remains to be elucidated.

FLNA is widely expressed in vascular smooth muscle cells (VSMCs), and regulates the structure and function of vascular smooth muscle (10). Specific deletion of FLNA in smooth muscle has been reported to markedly blunt the stretch activation of Cav1.2 and impair vascular wall tension, presenting as a decrease in arterial blood pressure (11). A previous proteomic analysis revealed that FLNA was significantly

upregulated in patients with congenital heart disease and irreversible PAH, and it was mainly located in pulmonary arterial smooth muscle cells (PASMCs) (12). However, the role of SMC-expressed FLNA in pulmonary vascular remodeling remains unclear. Therefore, the present study generated SMC-specific FLNA-knockout mice and aimed to investigate whether FLNA deficiency in SMCs protected mice from hypoxia-induced PAH and substantially ameliorated pulmonary vascular remodeling.

Materials and methods

Lung tissue samples. For experiments involving human tissues, approval was obtained from the Ethics Committees of Nanjing Medical University (approval no. KY20190505-09; Nanjing, China), and all subjects provided written informed consent before the study. The inclusion criteria included patients with idiopathic PAH who underwent lung transplantation at Wuxi People's Hospital (Wuxi, China); patients with other types of PAH were excluded. Between June 2019 and April 2020, lung samples were collected from three patients (age range, 28-40 years; two female patients and one male patient) with idiopathic PAH [mean pulmonary arterial pressure (PAP), 68.7±13.5 mmHg; pulmonary vascular resistance, 19.9±0.9 Woods units]. Three normal unused donor lungs (age range, 42-50 years; two women and one man) were used as controls.

Mice. SMC-specific FLNA-knockout mice were generated according to a previous study (11). All of the animals were housed at constant temperature (22±2°C) and relative humidity (50%) under a 12-h light/dark cycle, and were allowed *ad libitum* access to food and water. As FLNA is located on the X chromosome, 16 male Tagln-Cre^{ERT2} mice (Gempharmatech Co., Ltd.) were crossed with 32 female FLNA$^{flox/flox}$ mice (Gempharmatech Co., Ltd.) to generate 24 FLNA$^{flox/Y}$ Tagln-Cre^{ERT2+} mice (FLNA-CKO). Male mice aged 6 weeks old and weighing 18-22 g were used. A total of 24 FLNA$^{flox/Y}$ Tagln-Cre^{ERT2-} mice (FLNA-C; 6-week-old male mice; weight, 18-22 g) were used as controls. Tamoxifen (75 mg/kg; cat. no. T5648; MilliporeSigma) was intraperitoneally injected for 5 consecutive days to conditionally delete FLNA. On day 14 after the first tamoxifen injection, the mice were euthanized via overdose of pentobarbital sodium (200 mg/kg), and death was confirmed by cervical dislocation. FLNA expression was detected in the pulmonary artery and the aorta by reverse transcription-quantitative PCR (RT-qPCR) and immunohistochemical staining. In addition, DNA was extracted from tail clippings and the genotype was determined by PCR.

For tail genotyping, one 5-mm tail clipping was performed on each mouse <21 days of age without anesthesia. DNA was extracted from tail clippings using Animal Genomic DNA Quick Extraction Kit (cat. no. D0065S; Beyotime Institute of Biotechnology). The tail samples were lysed in lysis buffer containing DNA extraction solution and enzyme mix at 55°C for 15 min, followed by 95°C for 5 min. Subsequently, stop solution was added to stop the reaction. PCR was performed using the Quick Genotyping Assay Kit for Mouse Tail (cat. no. D7283S; Beyotime Institute of Biotechnology). The primer sequences were as follows: Wild-type FLNA, forward 5'-CCA AACTGAACCCGAAGAAA-3' and reverse 5'-TTTTGCCTC

TTCCTGGTGTC-3'; Cre, forward 5'-GCCTGCATTACC GGTCGATGC-3' and reverse 5'-CAGGGTGTTATAAGCA ATCCC-3'. The samples were amplified using the following thermocycling conditions: Initial denaturation at 95°C for 3 min; followed by 40 cycles of denaturation at 95°C for 30 sec, annealing at 55°C for 30 sec and elongation at 72°C for 30 sec; and final extension at 72°C for 10 min. Subsequently, PCR products were separated by 1% agarose gel electrophoresis, and the bands were stained in 20 mg/ml ethidium bromide for 15 min at room temperature and verified under an UV transilluminator. All of the experimental protocols were approved by the Institutional Animal Care and Use Committee of Nanjing Medical University (approval no. 1905004), and conformed with the National Institutes of Health guide for the care and use of laboratory animals (13).

Animal models. SU5416 is a selective vascular endothelial growth factor receptor inhibitor that may induce severe pulmonary hypertension if combined with chronic hypoxia. A commonly used protocol for the hypoxia/SU5416 model is 3 weeks hypoxic exposure, followed by 1 week normoxic exposure (14). However, several studies have argued that pulmonary hypertension may not be sustained after the hypoxic exposure has been discontinued (15,16). Therefore, in the present study, hypoxia exposure was prolonged to 4 weeks with weekly subcutaneous injections of 20 mg/kg SU5416 (cat. no. S8442; MilliporeSigma) (17). Briefly, 8-week-old male C57BL/6JGpt mice (weight, 22-24 g) were housed with *ad libitum* access to food and water at 22°C with 65% humidity and a 12-h light/dark cycle. The mice were subcutaneously injected with 20 mg/kg SU5416, and then exposed to chronic hypoxia (10% O$_2$) for the subsequent 4 weeks. Mice in the normoxic group were exposed to room air (10% O$_2$). A total of 36 mice were randomly divided into the following four groups (n=9/group): i) FLNA-C normoxic group; ii) FLNA-CKO normoxic group; iii) FLNA-C hypoxic group; and iv) FLNA-CKO hypoxic group.

Reagents. Antibodies against phosphorylated (p)-Akt (Ser473) (cat. no. 9271), Akt (cat. no. 9272), p-ERK (Thr202/Tyr204; cat. no. 9101), ERK (cat. no. 9102), p-PAK1 (Ser144; cat. no. 2606), PAK1 (cat. no. 2602) and proliferating cell nuclear antigen (PCNA; cat. no. 2586) were purchased from Cell Signaling Technology, Inc. Antibodies against FLNA (cat. no. ab76289), Ras-related C3 botulinum toxin substrate 1 (Rac1; cat. no. ab33186) and α-smooth muscle actin (α-SMA; cat. no. ab124964) were purchased from Abcam. Secondary antibodies used for western blotting were obtained from OriGene Technologies, Inc. (HRP-conjugated goat anti-rabbit IgG, cat. no. ZB-2301; HRP-conjugated goat anti-mouse IgG, cat. no. ZB-2305). Secondary antibodies used for immunofluorescence were obtained from OriGene Technologies, Inc. (TRITC-conjugated goat anti-rabbit IgG, cat. no. ZF-0316; FITC-conjugated goat anti-rabbit IgG, cat. no. ZF-0311). FLNA small interfering RNA (siRNA) (cat. no. sc-35374) and the control siRNA (cat. no. sc-37007) were purchased from Santa Cruz Biotechnology, Inc. pcDNA-myc-FLNA WT was obtained from John Blenis (Addgene #8982) (18). The control plasmid pcDNA™ 3.1$^{(+)}$ was purchased from Thermo Fisher Scientific, Inc. (cat. no. V79020).

Hemodynamic measurements. Right ventricular systolic pressure (RVSP) was measured as previously described (17). Before measurement, mice were intraperitoneally anesthetized with 45 mg/kg pentobarbital sodium. After RVSP was recorded, all mice were sacrificed by cardiac puncture under anesthesia and death was confirmed by cervical dislocation. Subsequently, the heart and lung tissues were removed. The right ventricle (RV) was separated from the left ventricle plus ventricular septum (LV + S). The weight ratio of RV/(LV + S) was calculated to assess the right ventricular hypertrophy index (RVHI).

Echocardiographic assessments. After anesthesia with 2% isoflurane, echocardiographic images were obtained with the Vevo 2100 imaging system (VisualSonics, Inc.). The following parameters were assessed: RV free wall thickness (RVWT), RV internal diameter (RVID), pulmonary artery acceleration time (PAAT) and pulmonary artery ejection time (PAET). The PAAT/PAET ratio was then calculated as an indirect measure of systolic PAP.

Histological, immunohistochemical and immunofluorescence analyses. The lung tissues were fixed in 10% neutral-buffered formalin for 24 h at room temperature followed by embedding in paraffin wax, and then cut into 5-μm slices. Paraffin-embedded slices were deparaffinized in xylene, rehydrated in a graded ethanol series to phosphate-buffered saline, and the slices were then stained with hematoxylin and eosin for 1 min, and elastic van Gieson for 3 min at room temperature, respectively.

For immunohistochemical staining, after deparaffinization and rehydration, antigen retrieval was performed by heat-mediated antigen retrieval with sodium citrate buffer (pH 6.0) at 95˚C for 3 min. Subsequently, the sections were stained with anti-FLNA (1:200) or anti-PCNA (1:2,000) primary antibodies at 4˚C overnight. Subsequently, the sections were incubated with biotinylated secondary antibody for 30 min at room temperature, followed by reaction with diaminobenzidine. The images were observed under an optical microscope (Olympus BX61; Olympus Corporation).

For immunofluorescence analysis, the slices were permeabilized with 0.3% Triton X-100 for 10 min and blocked by 1% bovine serum albumin (cat. no. ST023; Beyotime Institute of Biotechnology) for 1 h at room temperature. Then, primary antibodies against FLNA (1:200) and α-SMA (1:200) were applied at 4˚C overnight. The sections were then incubated with the respective secondary antibody at room temperature for 1 h, followed by DAPI counterstaining. Images were collected using laser scanning confocal microscopy (LSM 710; Carl Zeiss AG).

TUNEL staining. The mouse lung tissues were fixed in 10% neutral-buffered formalin for 24 h at room temperature. The TUNEL Apoptosis Assay kit (cat. no. C1098; Beyotime Institute of Biotechnology) was used to detect apoptotic cells in paraffin-embedded lung tissues, which were cut into 5-μm slices. The sections were deparaffinized and rehydrated, followed by incubation with 50 μl biotin labeling solution at 37˚C for 1 h in the dark. Subsequently, samples were incubated with 50 μl streptavidin-HRP solution for 30 min at room temperature and then with diaminobenzidine solution for

15 min at room temperature. The nuclei were counterstained with hematoxylin. The nuclei of positive cells were stained brown. The positively stained cells in five different fields of view were observed under an optical microscope (Olympus BX61; Olympus Corporation). The cell apoptotic rate was calculated as the percentage of TUNEL-positive cells.

Cell culture. Human pulmonary arterial smooth muscle cells (HPASMCs; cat. no. 3110) were obtained from ScienCell Research Laboratories, Inc. and cells at passages 4-9 were used for the present study. The cells were cultured with complete smooth muscle cell medium (cat. no. 1101; ScienCell Research Laboratories, Inc.) at 37˚C in a 5% CO_2-humidified incubator. Ethics approval for the use of HPASMCs was obtained from the Ethics Committees of the Nanjing Medical University. FLNA was knocked down and overexpressed in HPASMCs to investigate the effects of FLNA on cell proliferation and migration. FLNA was knocked down using siRNA and was overexpressed by transfection with overexpression plasmids. PASMCs were seeded into 6-well culture plates and when the cells had reached 70% confluence, they were transfected with FLNA siRNA (50 nmol/l), control siRNA (50 nmol/l), pcDNA-myc-FLNA WT (2 μg) or control plasmid (2 μg) per well under serum-free conditions using Lipofectamine® 2000 (Invitrogen; Thermo Fisher Scientific, Inc.). After 6 h at 37˚C, the infection solution was replaced by complete medium. After transfection for 48 h, cells were harvested for further analysis.

Proliferation assays. PASMC viability and proliferation was assessed using Cell Counting Kit 8 (CCK-8) and EdU staining assays. For the CCK-8 assay, a cell suspension was prepared and $2x10^3$ cells/well in 100 μl medium was added into 96-well plates. CCK-8 (cat. no. C0038; Beyotime Institute of Biotechnology) solution was added to the 96-well plate and incubated at 37˚ for 3 h. Absorbance was determined at a wavelength of 450 nm.

For the EdU staining assay, PASMCs were seeded at a density of $1x10^5$ cells/well in a 6-well plate. After transfection for 48 h, the cells were incubated with 10 μM EdU (Beyotime Institute of Biotechnology, cat. no. C0071S) for 2 h at 37˚C. Then, the cells were fixed in 4% paraformaldehyde for 15 min at room temperature and permeabilized by 0.3% Triton X-100 in PBS at room temperature for 15 min. Finally, click reaction cocktail was added to inactivate endogenous peroxidase for 30 min at room temperature in the dark. Cell nuclei were stained with DAPI and images were captured via fluorescence microscopy. Proliferation was expressed as the percentage of EdU-positive cells.

Migration assays. Transwell migration and wound-healing assays were used to assess PASMC migration (19). For the wound-healing assay, PASMCs were seeded into 6-well plates until the cell density approached 90%. A sterile 10-μl pipette tip was used to produce a straight scratch to the cell monolayer and the cells were then incubated with serum-free medium. Migration was determined as the percentage of the wound closure; images were captured at 0 and 24 h under an optical microscope.

For the Transwell assay, the cells were seeded in the Transwell chamber (cat. no. CLS3428; Corning, Inc.) located in a 24-well plate. Subsequently, $1x10^5$ cells in 200 μl

serum-free medium were seeded in the upper chamber and 600 μl complete medium containing 20% FBS was added to the lower chamber. The cells were cultured for 24 h at 37°C. Then, the cells on the upper membrane surface were removed, whereas the cells that had migrated to the lower membrane surface were fixed with 4% paraformaldehyde for 30 min, and then stained with crystal violet for 30 min at room temperature. Finally, the number of cells in five random fields on each membrane was counted under a light microscope.

RT-qPCR. Total RNA was isolated using RNA isolater Total RNA Extraction Reagent (cat. no. R401-01; Vazyme, Inc.) from the PASMCs and mouse tissues, and RT was performed usig the HiScript II Q Select RT SuperMix (cat. no. R232-01; Vazyme, Inc.) at 50°C for 15 min and terminated at 85°C for 5 sec. qPCR was carried out using Taq Pro Universal SYBR qPCR Master Mix (cat. no. Q712-02; Vazyme, Inc.). The reference genes were β-actin for human PASMCs and GAPDH for mouse lung tissues. PCR amplification was performed as follows: Initial denaturation at 95°C for 3 min; followed by 40 cycles of denaturation at 95°C for 30 sec, annealing at 55°C for 30 sec and elongation at 72°C for 30 sec. The primers used were as follows: FLNA (human), forward 5'-CAGTGCTAT GGGCCTGGTAT-3', reverse 5'-CCACTTTGTACATGCCAT CG-3'; β-actin (human), forward 5'-AAACGTGCTGCTGAC CGAGR-3', reverse 5'-TAGCACAGCCTGGATAGCAAC-3'; FLNA (mouse), forward 5'-CCAAACTGAACCCGAAGA AA-3', reverse 5'-TTTTGCCTCTTCCTGGTGTC-3', GAPDH (mouse), forward 5'-AGGTCGGTGTGAACGGATTTG-3', reverse 5'-TGTAGACCATGTAGTTGAGGTCA-3'. Results were qualified using the $2^{-\Delta\Delta Cq}$ method (20).

Western blotting. Total protein was extracted from the tissues and PASMCs with RIPA buffer (cat. no. P0013B; Beyotime Institute of Biotechnology) containing protease and phosphatase inhibitor cocktail (cat. no. P1046; Beyotime Institute of Biotechnology). Protein concentration was measured using the bicinchoninic acid method (cat. no. P0010S; Beyotime Institute of Biotechnology) and 50 μg protein/lane was separated by SDS-PAGE on 8-12% gels. The proteins were subsequently transferred to PVDF membranes, which were blocked with 10% milk for 1 h at room temperature and incubated overnight at 4°C with the primary antibodies (1:2,000 for FLNA; 1:1,000 for other proteins). The membranes were subsequently incubated with the corresponding secondary antibody (1:1,000) for 2 h at 37°C and were detected using the enhanced chemiluminescence system (cat. no. P0018S; Beyotime Institute of Biotechnology). The bands were semi-quantified using Quantity One version 4.6.6 software (Bio-Rad Laboratories, Inc.).

Rac1 activation assay. The degree of activation of Rac1 was measured using a G-LISA Ras Activation Assay Biochem kit (cat. no. BK131; Cytoskeleton, Inc.) according to the manufacturer's instructions (21).

Statistical analysis. All continuous variables are presented as the mean ± SD. At least three repeats were performed for each experiment. Unpaired Student's t-test was used to determine the statistical difference between two groups. Differences between multiple groups were compared with one-way ANOVA followed by Bonferroni's post hoc test. All analyses were performed using SPSS version 22.0 (IBM Corporation). P<0.05 was considered to indicate a statistically significant difference.

Results

FLNA is significantly upregulated in the pulmonary arteries of patients with PAH. As determined by western blotting and immunofluorescence staining, the expression levels of FLNA were markedly increased in lung tissues from patients with PAH compared with in control individuals (Fig. 1). FLNA was mainly expressed in the PASMCs of pulmonary arterioles, as evidenced by α-SMA co-immunostaining (Fig. 1C). These results suggested that FLNA may be an important factor in pulmonary vascular remodeling.

Generation of SMC-specific FLNA-knockout mice. As FLNA-knockout mice exhibit embryonic lethality (22), the female FLNA$^{flox/flox}$ mice were crossed with male Tagln-Cre^{ERT2+} mice to produce male hemizygote FLNA$^{flox/Y}$ Tagln-Cre^{ERT2+} mice (Fig. 2A). Using PCR, the presence of floxed alleles and Cre recombinase was detected in male FLNA$^{flox/Y}$ hemizygotes. The FLNA$^{flox/Y}$ mice without the Cre recombinase were used as controls (Fig. 2B). SMC-specific FLNA deficiency (FLNA-CKO) was induced in 8-week-old FLNA$^{flox/Y}$ Tagln-Cre^{ERT2+} mice by intraperitoneal injection of tamoxifen for 5 consecutive days, and FLNA depletion was confirmed by RT-qPCR and immunohistochemical staining at day 14 after the initial tamoxifen injection. RT-qPCR analysis of the aorta and pulmonary artery demonstrated a significant decrease in FLNA expression in FLNA-CKO mice (Fig. 2D). Immunohistochemical staining further confirmed the downregulation of FLNA in the aorta and pulmonary artery (Fig. 2C). These results indicated that tamoxifen efficiently induced FLNA deficiency in vascular smooth muscle cells. Furthermore, TUNEL staining suggested that the apoptotic rate was significantly increased in FLNA-CKO mice (Fig. S1).

FLNA deficiency alleviates PAH in the hypoxia/SU5416 mouse model. After exposure to hypoxia, the RVSP was significantly increased in the hypoxic groups of both FLNA-C and FLNA-CKO mice. However, compared with in FLNA-C mice, FLNA-CKO mice exhibited a significantly lower RVSP (Fig. 3A and B). In addition, RVHI was much lower in FLNA-CKO mice than that in FLNA-C mice after hypoxic exposure (Fig. 3C). Echocardiography revealed that RV dilatation and RV thickness were attenuated in FLNA-CKO mice after hypoxic exposure (Fig. 3D and E). Moreover, right heart function after exposure to chronic hypoxia was improved in FLNA-CKO mice, as revealed by PAAT/PAET ratio (Fig. 3F).

Histological studies revealed that FLNA-CKO could ameliorate pulmonary vascular remodeling. The medial wall thickness and medial wall area were increased after hypoxia exposure, and were significantly decreased in FLNA-CKO mice compared with those in FLNA-C mice (Fig. 3G and H). Immunofluorescence staining confirmed that FLNA was mainly expressed in α-SMA-positive SMCs in pulmonary arterioles; FLNA expression was increased in α-SMA-positive smooth muscle cells after hypoxic exposure, but was markedly
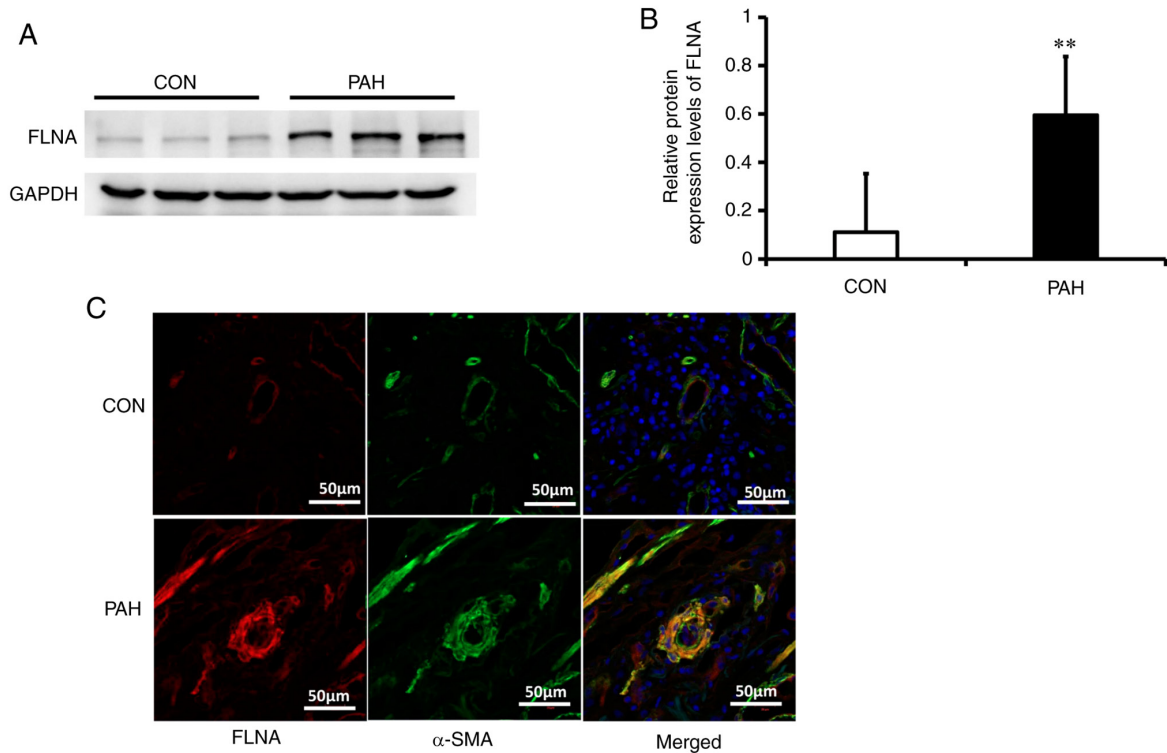
Figure 1. FLNA expression and location in the pulmonary arterioles of patients with IPAH. (A) Representative bands of FLNA expression in patients with IPAH and control individuals. GAPDH was used as a loading control. (B) Semi-quantification results of FLNA expression levels with GAPDH as the control. (C) Immunofluorescence staining of FLNA and α-SMA in patients with IPAH, scale bars indicate 50 μm. Data are presented as the mean ± SD, n=3/group. **P<0.01 vs. control group. α-SMA, α-smooth muscle actin; IPAH, idiopathic pulmonary arterial hypertension; FLNA, filamin A.
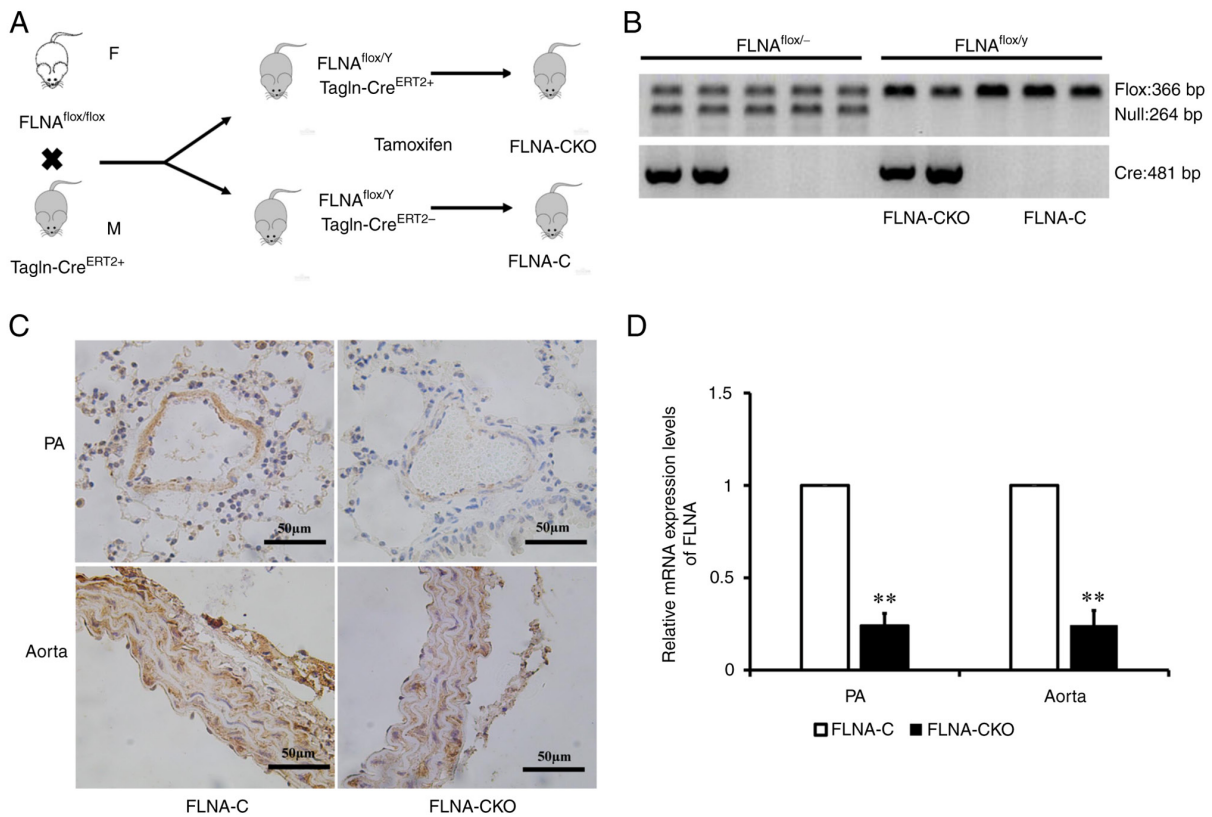

Figure 2. Generation of smooth muscle cell-specific FLNA-CKO mice. (A) Schematic diagram of transgenic mice used to generate FLNA-CKO and FLNA-C mice. (B) PCR analysis of tail genomic DNA to determine the presence of the floxed and null alleles. (C) Immunohistochemical analysis to confirm FLNA depletion in PA and aorta tissues, scale bars indicate 50 μm. (D) mRNA expression levels of FLNA in the PA and aorta were determined by reverse transcription-quantitative PCR (n=4 mice/group). Data are presented as the mean ± SD. **P<0.01 vs. FLNA-C. FLNA-C, FLNAflox/Y Tagln-CreERT2- mice; FLNA-CKO, FLNAflox/Y Tagln-CreERT2+ mice; FLNA, filamin A; PA, pulmonary artery.
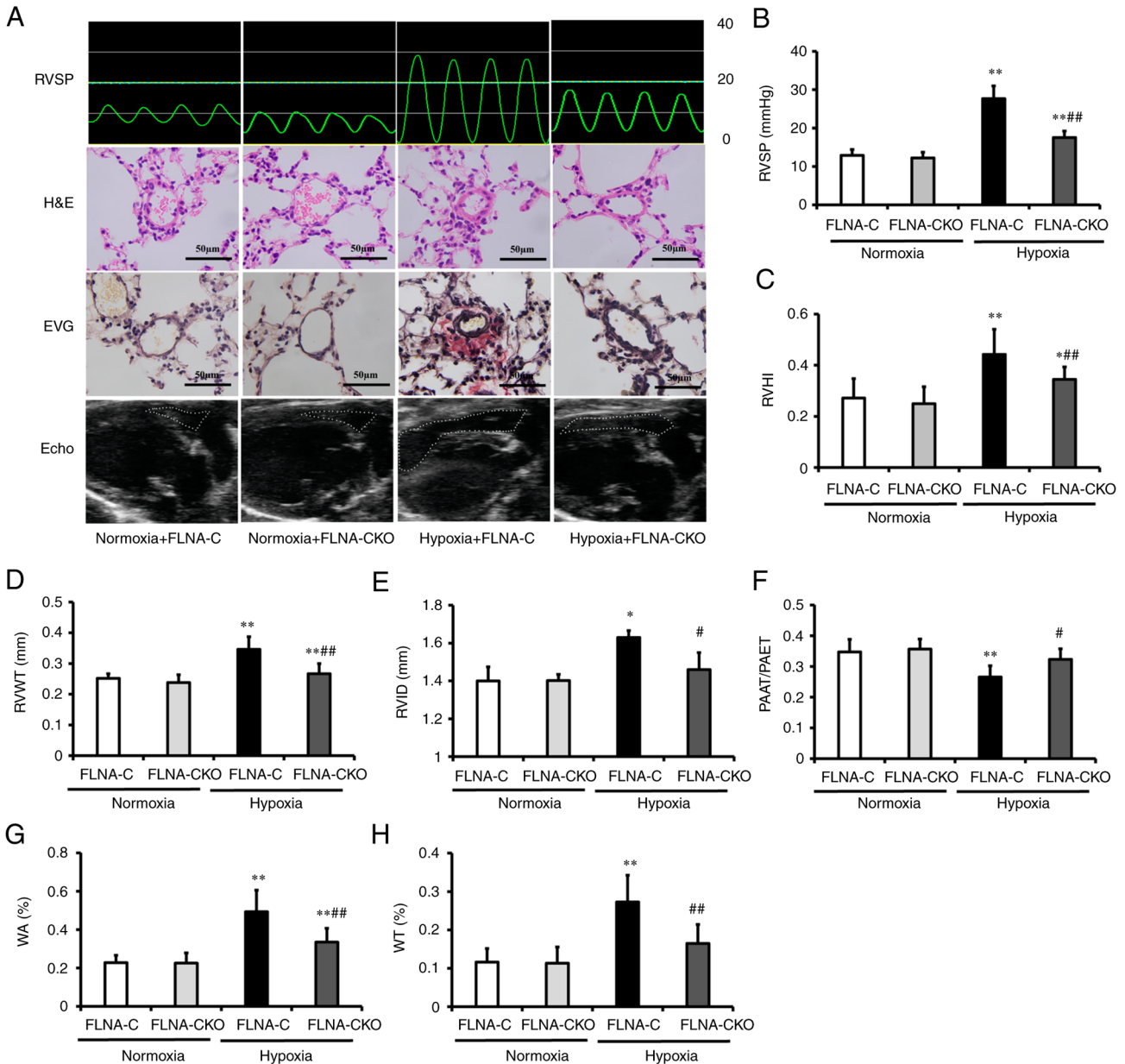
Figure 3. FLNA deficiency in smooth muscle cells alleviates pulmonary arterial hypertension after exposure to hypoxia. (A) Representative images of RVSP, lung H&E and EVG staining, and echocardiography in hypoxia/SU5416 mice, scale bars indicate 50 μm. (B) Hemodynamic measurements revealed decreased RVSP in FLNA-CKO mice after hypoxia exposure. (C) RVHI was alleviated in FLNA-CKO mice after hypoxia exposure. (D) RVWT, (E) RVID and (F) PAAT/PAET ratio were measured by echocardiography. (G) WA and (H) WT changes in FLNA-CKO mice after hypoxia exposure. Data are presented as the mean ± SD, n=9/group. *$P<0.05$ and **$P<0.01$ vs. FLNA-C normoxic group; #$P<0.05$ and ##$P<0.01$ vs. FLNA-C hypoxic group. EVG, elastic van Gieson; FLNA-C, FLNAflox/Y Tagln-CreERT2- mice; FLNA-CKO, FLNAflox/Y Tagln-CreERT2+ mice; FLNA, filamin A; H&E, hematoxylin and eosin; PAAT, pulmonary artery acceleration time; PAET, pulmonary artery ejection time; RVHI, right ventricular hypertrophy index; RVWT, right ventricular wall thickness; RVID, right ventricular internal diameter; RVSP, right ventricular systolic pressure; WA, wall area; WT, wall thickness.

decreased in FLNA-CKO compared with in FLNA-C mice (Fig. 4A). Immunohistochemical analyses also revealed that FLNA knockout significantly inhibited hypoxia-induced PASMC proliferation, as evidenced by a reduction in the number of PCNA-positive cells (Fig. 4B and C). Thus, loss of FLNA in SMCs may confer protective effects in hypoxia-induced pulmonary vascular remodeling and PASMC hyperplasia.

Knockdown of FLNA impairs PASMC proliferation and migration. In *in vitro* studies, FLNA siRNA was used to knockdown FLNA expression. The efficient knockdown of FLNA in PASMCs was identified by western blotting (Fig. 5A and B)

and RT-qPCR (Fig. 5C). Both CCK-8 and EdU staining assays indicated that FLNA knockdown significantly inhibited PASMC viability and proliferation, respectively (Fig. 5D-F). Similarly, Transwell migration and wound-healing assays demonstrated a marked effect of FLNA knockdown on the migration of PASMCs; PASMC migration was significantly decreased in the FLNA siRNA-treated group compared with that in the control group (Fig. 5G-J).

To determine the molecular mechanisms behind the FLNA knockdown-induced decreases in cell proliferation and migration, the expression levels of downstream signaling molecules, including p-PAK1, p-AKT, p-ERK and Rac1, were
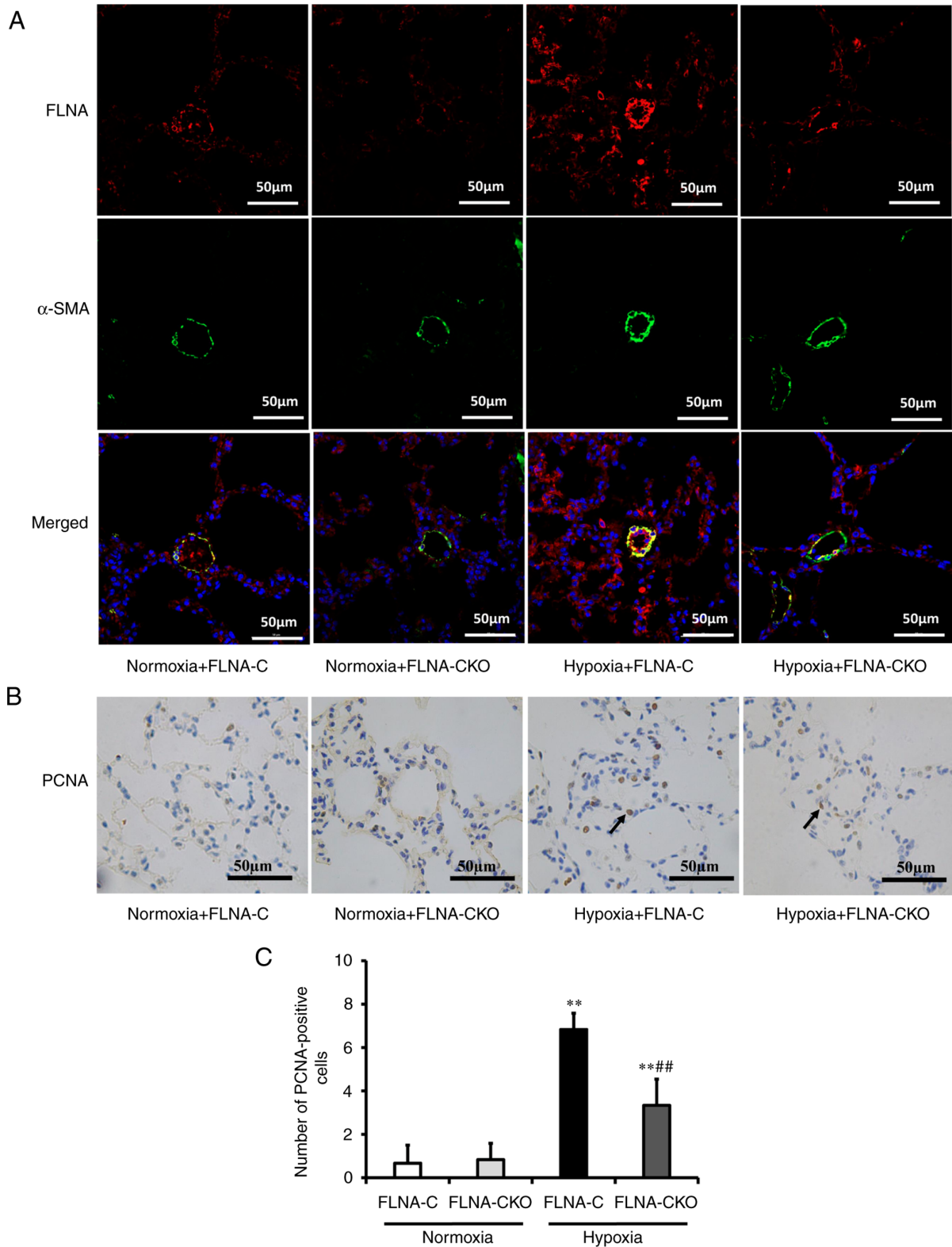
Figure 4. FLNA and PCNA expression in FLNA-CKO mice after exposure to hypoxia. (A) Representative optical sections (confocal microscopy) demonstrated FLNA-positive or α-SMA-positive cells in pulmonary arteries of FLNA-CKO mice after hypoxia exposure, scale bars indicate 50 μm. (B) PCNA staining was used to indicate pulmonary artery smooth muscle cell proliferation in pulmonary arterioles. (C) Number of PCNA-positive cells in pulmonary arterioles. The arrows indicate PCNA positive cells. [**]P<0.01 vs. FLNA-C normoxic group; [##]P<0.01 vs. FLNA-C hypoxic group. α-SMA, α-smooth muscle actin; FLNA-C, FLNAflox/Y Tagln-CreERT2- mice; FLNA-CKO, FLNAflox/Y Tagln-CreERT2+ mice; FLNA, filamin A; PCNA, proliferating cell nuclear antigen.

determined. FLNA siRNA-transfected PASMCs exhibited significantly reduced p-PAK1 levels (Fig. 6A and B); however, there was no change in p-AKT, p-ERK and Rac1 expression (Fig. 6A and C-E). BY contrast, G-LISA assay revealed that Rac1 activity was decreased by 56% in PASMCs transfected with FLNA siRNA (Fig. 6F).
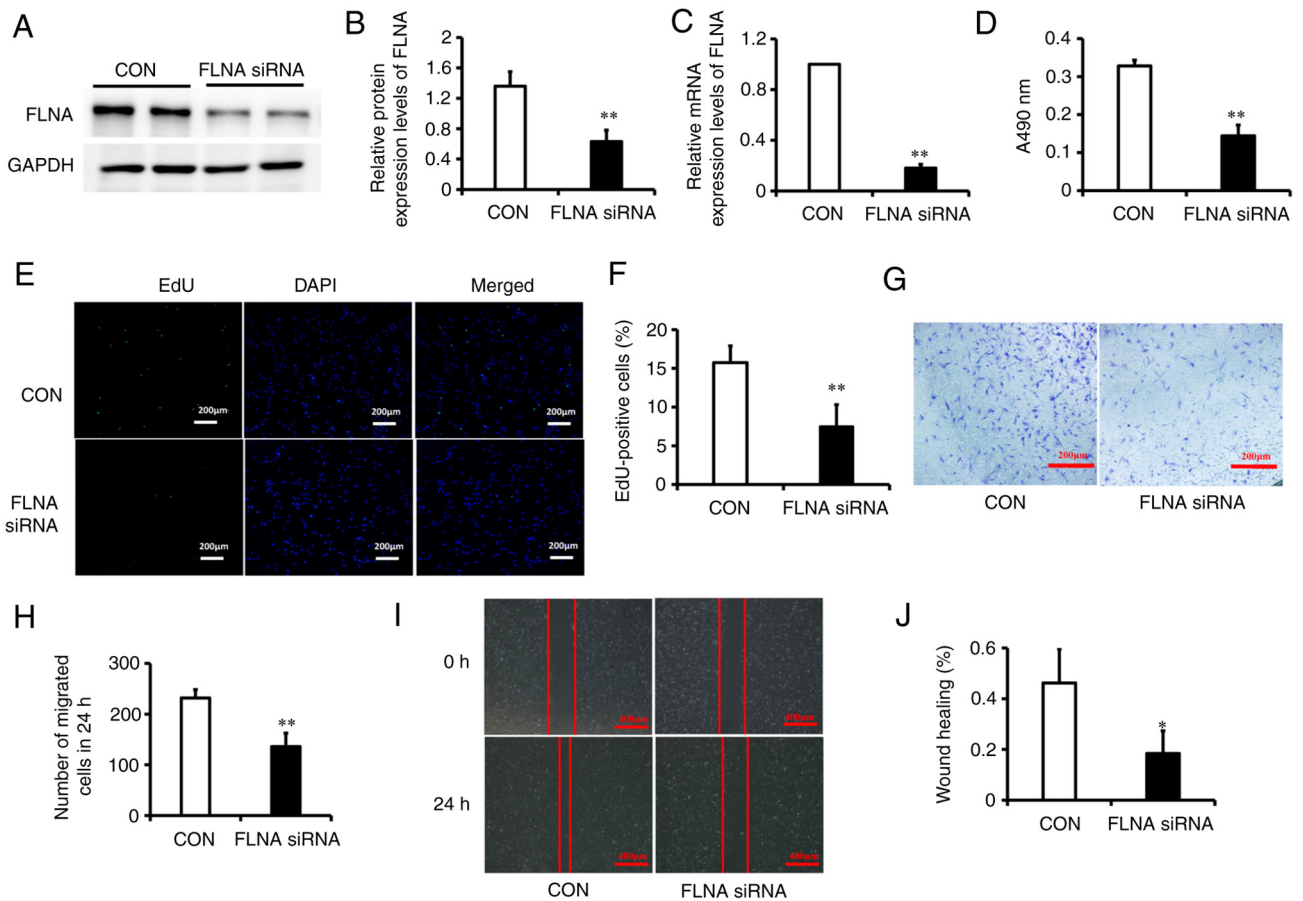
Figure 5. FLNA knockdown inhibits proliferation and migration of PASMCs. (A) Representative western blots of FLNA and GAPDH in control or FLNA siRNA-transfected PASMCs. (B) Statistical analysis of relative protein expression levels. (C) mRNA expression levels of FLNA were determined by reverse transcription-quantitative PCR. (D) Cell Counting Kit 8 analysis of PASMCs transfected with FLNA siRNA. (E) EdU staining. (F) Number of EdU-positive cells. (G) Transwell migration assay. (H) Number of migrated cells. (I) Wound-healing assay. (J) Percentage of wound healing. Data are presented as the mean ± SD, n=4-6 replicates/group. $^{*}P<0.05$ and $^{**}P<0.01$ vs. control group transfected with control siRNA. FLNA, filamin A; PASMCs, pulmonary artery smooth muscle cells; siRNA, small interfering RNA.

FLNA overexpression promotes PASMC proliferation and migration. FLNA overexpression was achieved by transfection with FLNA plasmids, and confirmed by western blotting (Fig. 7A and B) and RT-qPCR (Fig. 7C). The CCK-8 and EdU proliferation assays showed that PASMC viability and proliferation was significantly higher in FLNA plasmid-transfected cells compared with that in the control group (Fig. 7D-F). Similarly, the results of the migration assays confirmed a significant increase in PASMC migration after FLNA overexpression (Fig. 7G-J). Moreover, western blotting revealed that p-PAK1 levels were significantly increased in cells transfected with the FLNA plasmid (Fig. 8A and B); however, there was no change in p-AKT, p-ERK and Rac1 expression (Fig. 8A and C-E). Furthermore, G-LISA assay revealed that Rac1 activity was increased in PASMCs transfected with the FLNA plasmid (Fig. 8F). These findings indicated that FLNA overexpression induced PASMC proliferation and migration, whereas FLNA knockdown suppressed the proliferation and migration of these cells.

Discussion

The present study demonstrated that FLNA was significantly increased in the lung tissue of patients with PAH and it was mainly located in PASMCs. Subsequently, SMC-specific FLNA-knockout mice were generated and it was revealed that FLNA deficiency in SMCs markedly protected mice from hypoxia-induced PAH and alleviated pulmonary vascular remodeling. *In vitro* studies suggested that FLNA overexpression induced PASMC proliferation and migration, whereas knockdown of FLNA inhibited cell proliferation and migration. In addition, PAK1 signaling was revealed to be affected by the knockdown and overexpression of FLNA, suggesting that PAK1 may act as a downstream signaling pathway of FLNA. These findings demonstrated that FLNA deficiency in PASMCs alleviated PAH by impairing PASMC proliferation and migration. Notably, the present study may improve the understanding of the function of FLNA in pulmonary vascular remodeling.

Mutations in FLNA can cause variable clinical features, including neurological, skeletal and cardiac dysfunction. Several reports have indicated that patients with FLNA mutations present with severe diffuse lung disease and severe pulmonary hypertension (23,24). Masurel-Paulet *et al* (25) reported that a male patient with a mosaic nonsense FLNA mutation presented with PAH and severe lung manifestations, and lung histology showed pan-pulmonary emphysema with a marked reduction of bronchial cartilage. Hirashiki *et al* (9)
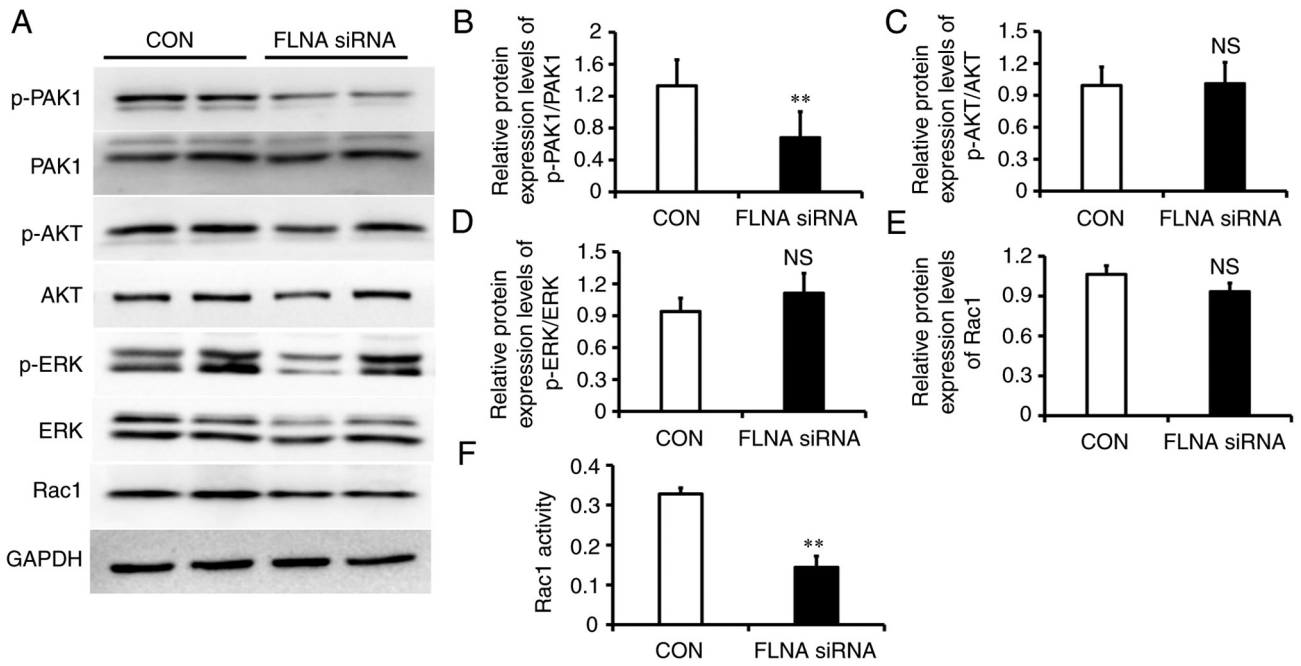
Figure 6. Impaired cell signaling in PASMCs lacking FLNA. (A) Representative western blots of p-PAK1, PAK1, p-Akt, Akt, p-ERK, ERK and Rac1. GAPDH was used as a loading control. Statistical analysis of relative protein expression levels of (B) p-PAK1/PAK1, (C) p-AKT/AKT, (D) p-ERK/ERK and (E) Rac1. (F) Rac1 activity was measured by G-LISA. Data are presented as the mean ± SD, n=4/group. **P<0.01 vs. control group. FLNA, filamin A; NS, not significant; p-, phosphorylated; PASMCs, pulmonary artery smooth muscle cells; Rac1, Ras-related C3 botulinum toxin substrate 1; siRNA, small interfering RNA.
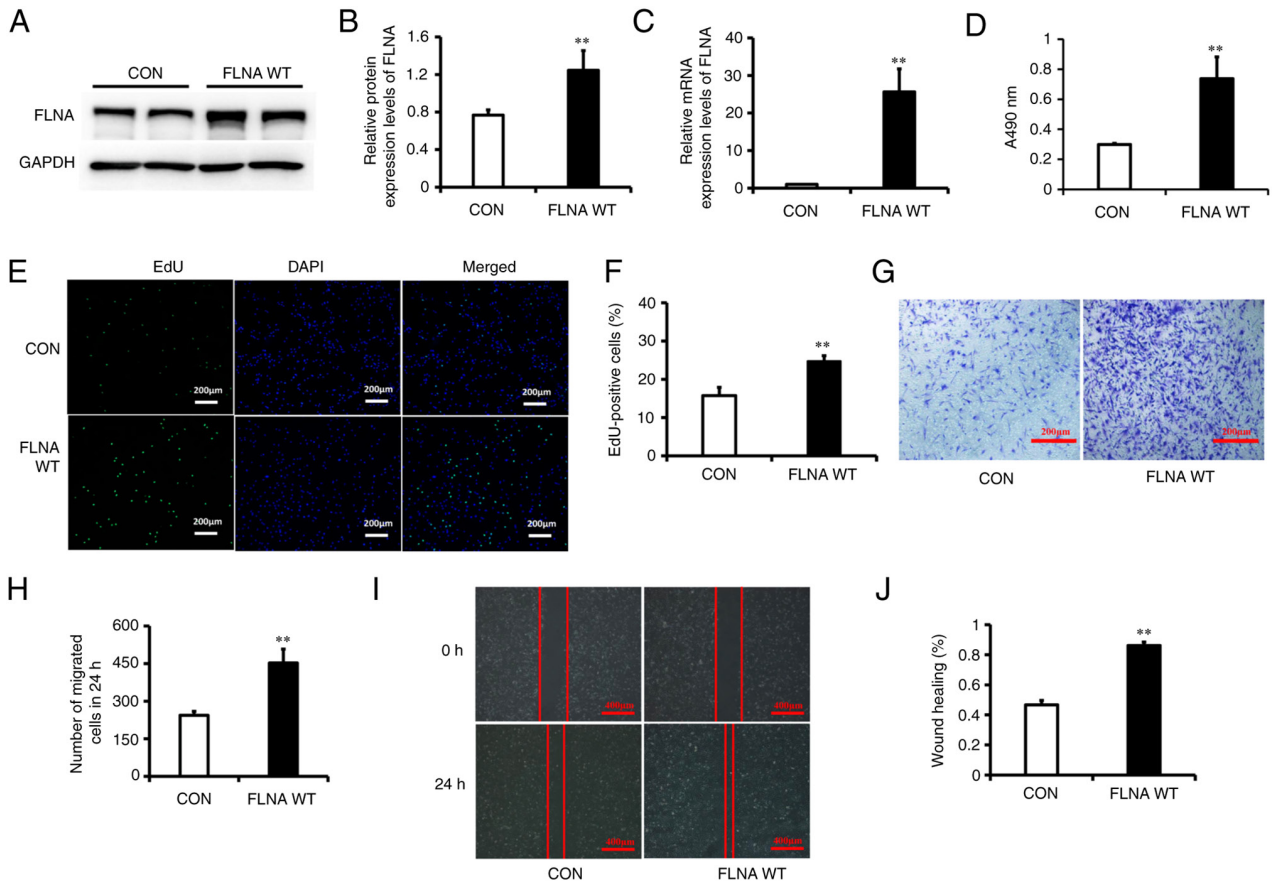

Figure 7. FLNA overexpression promotes proliferation and migration of PASMCs. (A) Representative western blots of FLNA and GAPDH in PASMCs transfected with control or FLNA overexpression plasmids. (B) Statistical analysis of relative protein expression levels. (C) mRNA expression levels of FLNA were determined by reverse transcription-quantitative PCR. (D) Cell Counting Kit 8 analysis of PASMCs transfected with a FLNA plasmid. (E) EdU staining. (F) Number of EdU-positive cells. (G) Transwell migration assay. (H) Number of migrated cells. (I) Wound-healing assay. (J) Percentage of wound healing. Data are presented as the mean ± SD, n=4-6/group. **P<0.01 vs. control group. FLNA, filamin A; PASMCs, pulmonary artery smooth muscle cells; siRNA, small interfering RNA; WT, wild type.
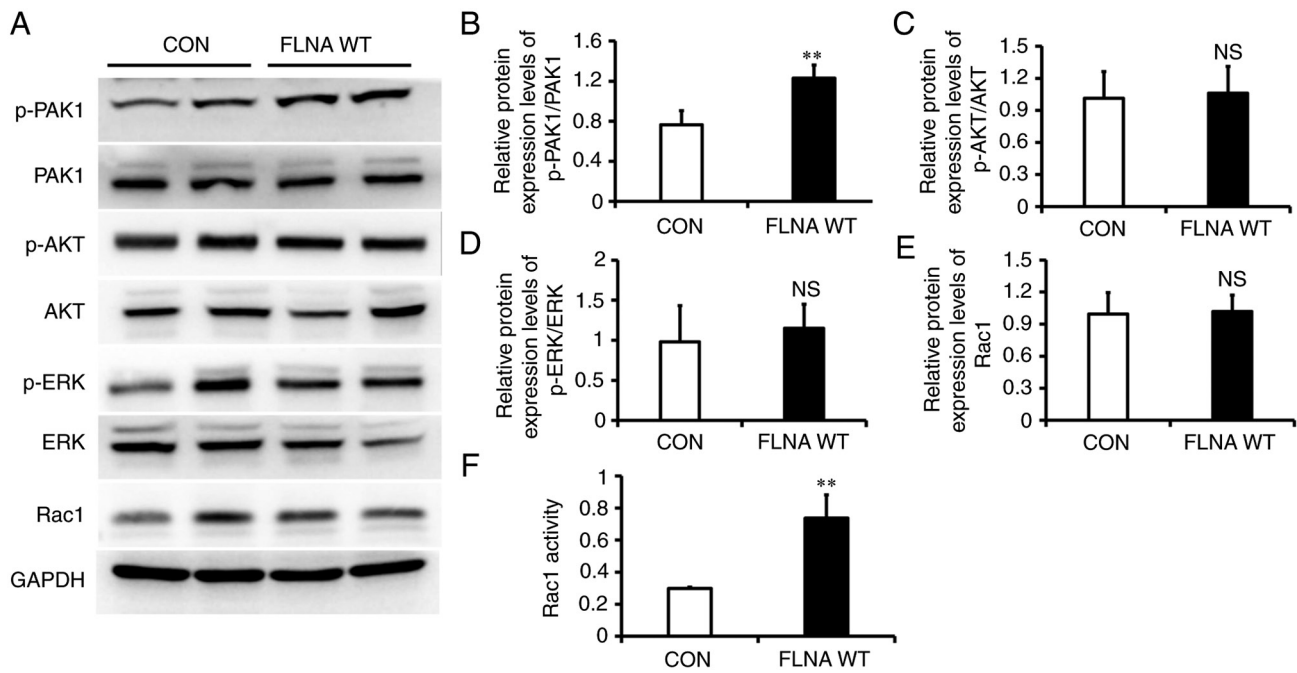
Figure 8. PAK1 and Rac1 activation in PASMCs overexpressing FLNA. (A) Representative western blots of p-PAK1, PAK1, p-Akt, Akt, p-ERK, ERK and Rac1. GAPDH was used as a loading control. Statistical analysis of relative protein expression levels of (B) p-PAK1/PAK1, (C) p-AKT/AKT, (D) p-ERK/ERK and (E) Rac1. (F) Rac1 activity was measured by G-LISA. Data are presented as the mean ± SD, n=4/group. **P<0.01 vs. control group. FLNA, filamin A; NS, not significant; p-, phosphorylated; PASMCs, pulmonary artery smooth muscle cells; Rac1, Ras-related C3 botulinum toxin substrate 1; WT, wild type.

reported that a family with heritable PAH carried a novel heterozygous splicing mutation in the FLNA gene. Deng *et al* (23) summarized 19 pediatric cases with FLNA mutation; these patients presented with early onset PAH and all cases were complicated with congenital heart disease. Sasaki *et al* (26) summarized 18 cases of FLNA mutation and interstitial lung disease (ILD), 14 of which had PAH. These findings indicated that ILD may lead to PAH, but not all patients with FLNA mutations present with ILD. Furthermore, concomitant congenital heart disease may also affect our understanding of the real cause of rapidly progressive PAH in patients with FLNA mutations. Therefore, the role of FLNA in PAH needs to be further investigated.

The present study demonstrated that FLNA was upregulated in the lung tissue of patients with PAH and that enhanced FLNA expression was predominantly located in PASMCs. This finding was in accordance with that of a previous study where FLNA was obviously increased in the lung tissues of patients with congenital heart disease and irreversible PAH (CHD-PAH) (12). Increased FLNA in irreversible CHD-PAH indicated that pulmonary arteriolar cells were in a state of hyperproliferation. In addition, FLNA is expressed in human cancer, and can promote cancer cell growth and angiogenesis (27). As the vascular lesions of PAH exhibit some cancer-like characteristics, it was hypothesized that FLNA may have a similar effect on promoting PASMC proliferation and reducing apoptosis.

FLNA was originally isolated from chicken gizzard VSMCs and it was revealed to interact with multiple transmembrane proteins (28,29). FLNA physically links the integrin receptors and VSMC contractile filaments, and is involved in regulating vascular integrity (30). Yu *et al* (31) demonstrated that FLNA was involved in regulating the

spreading and migration of VASMCs through binding with the P2Y2 receptor. Pena *et al* (32) reported that tissue factor could induce FLNA Ser-2152 phosphorylation, upregulate downstream small G-proteins Cdc42, RhoA and Rac1 protein expression, and significantly promote the migration of coronary artery smooth muscle cells. Because global knockout of FLNA is embryonically lethal, the present study generated mice with tamoxifen-inducible SMC-specific knockout of FLNA. Following exposure to hypoxia, FLNA-deficient mice displayed significantly reduced RVSP and attenuated pulmonary vascular remodeling. To further investigate the mechanisms by which FLNA regulates pulmonary vascular remodeling, the present study examined the effects of FLNA knockdown and overexpression on the proliferation and migration of cultured PASMCs. The results revealed that FLNA knockdown reduced PASMC proliferation and migration, whereas FLNA overexpression promoted cell proliferation and migration. Retailleau *et al* (33) revealed that deletion of FLNA in VSMCs resulted in enhanced arterial compliance and lower blood pressure, culminating in aortic dilation. Loss of smooth muscle FLNA has been shown to impair pressure-dependent calcium influx and attenuate the arterial myogenic tone (11). The myogenic response of small arteries is intricately linked to changes in wall structure. These studies suggested that FLNA was involved in SMC proliferation and migration, and served a key role in maintaining arterial myogenic tone and vascular remodeling in PAH. Unfortunately, the systemic blood pressure was not measured in the animal model used in the present study, and this may be a limitation of the present study.

The role of FLNA in the cellular response to hypoxia may be complex. Hypoxia induces calpain-dependent cleavage of FLNA to generate a naturally occurring C-terminal fragment that accumulates in the cell nucleus (27). Increased C-terminal
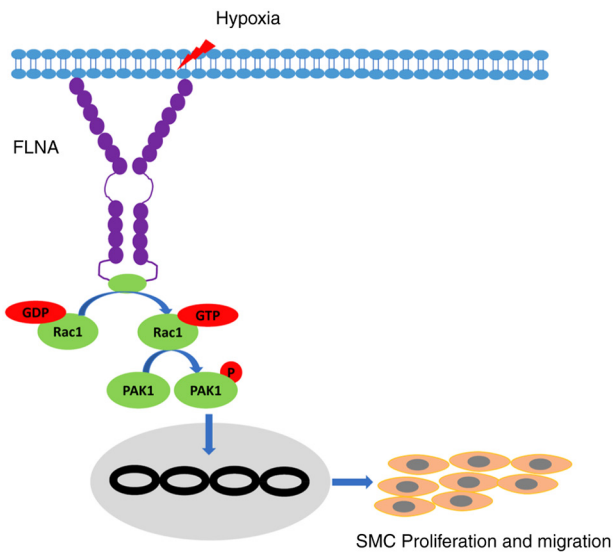
Figure 9. Schematic overview of the proposed mechanisms for FLNA/PAK1 signaling pathway in PAH. FLNA, filamin A; Rac1, Ras-related C3 botulinum toxin substrate 1; SMC, smooth muscle cell.

fragment could facilitate the expression of several transcription factors, including AP-1 and HIF-1α. AP-1 is a transcription factor that regulates FLNA expression (34), and HIF-1α can potentiate angiogenesis and tumor progression (27). In addition to upregulation of calpain activity, hypoxia may have an effect on the phosphorylation status of FLNA, thus promoting the activation of several downstream kinases, including PKA, PAK1 and RSK (35). Further studies are necessary to address this question.

The present study also examined the changes in downstream signaling pathways. FLNA knockdown was achieved by transfection with FLNA siRNA, whereas FLNA overexpression was produced using a FLNA plasmid. Notably, as the difference in molecular weight between myc-FLNA and FLNA is too slight, it is difficult to discriminate FLNA and myc-FLNA fusion proteins in western blotting; therefore, FLNA was detected in the present study. The present results revealed that p-PAK-1 and Rac1 activity were increased after FLNA overexpression, whereas p-PAK-1 and Rac1 activity were attenuated by FLNA knockdown. FLNA binding to Rac1 and Cdc42 stimulates PAK1 kinase activity and thus leads to cytoskeletal reorganization (36). Rac1 is a member of the subfamily of small G-protein superfamily, and it is involved in the formation of cytoskeletal networks. Rac1 activation has been observed in both patients with PAH and animal models of PAH, and it has been reported to be correlated with the severity of PAH (37). Dilasser et al (38) demonstrated that Rac1 activation was essential for hypoxia-induced PASMC proliferation and Rac1 deletion in SMCs inhibited hypoxia-induced pulmonary arterial remodeling and reactive oxygen species production. Furthermore, bone morphogenetic protein receptor 2 (BMPR-2) gene mutations can activate RhoA and Rac1, suggesting that RhoA and Rac1 act as downstream signals of BMPR-2 (39). The present study also revealed that only Rac1 activity, but not expression, was affected following treatment. Similarly, Kim et al (40) reported that FLNA was required for Rac1 activation in the invasion of gastric cancer

cells, and depletion of FLNA expression markedly reduced Rac1 activity. It was hypothesized that FLNA could serve as a scaffold protein that mediates Rac1 activation, whereas it had no effect on Rac1 gene transcription and protein expression. Therefore, small G-protein Rac1 may act as an important ligand that is involved in FLNA-mediated PASMC proliferation and migration.

PAK1 is the main downstream target protein of Cdc42 and Rac1 small G-proteins, and participates in regulating cell migration, apoptosis and cytoskeleton recombination. PAK1 is widely expressed in VSMCs and numerous studies have reported that PAK1 activation is involved in vascular remodeling (41). In vitro studies suggested that PAK1 was involved in both angiotensin II- and platelet-derived growth factor-mediated VSMC migration and proliferation (41). Further in vivo studies revealed that PAK1 was activated in the rat carotid artery balloon injury model; inactivation of PAK1 attenuated SMC migration from the media to intima, contributing to reduced neointima formation and increased lumen size (42). Fediuk et al (43) revealed that hypoxia increased PAK1 phosphorylation via Cdc42 and inhibition of PAK1 prevented hypoxia-induced actin polymerization. PAK1 and Rac1 have been shown to be expressed in the media of remodeled pulmonary vessels, and activation of PAK1 can promote PASMC proliferation through stimulating HIF activity and HIF-1α expression (44). Therefore, PAK1 may serve a major role in the pathogenesis of pulmonary vascular remodeling, and Rac1 and PAK1 inhibitors may be potential drugs for PAH therapy. It was hypothesized that FLNA activated downstream PAK1 by acting on its ligand small G-protein Rac1, leading to the proliferation and migration of PASMCs, and finally contributing to pulmonary vascular remodeling and pulmonary hypertension (Fig. 9). However, the direct relationship between Rac1 and PAK1, and their functional roles in PASMC proliferation and migration were not established and require further confirmation.

In conclusion, the present study demonstrated that FLNA expression was elevated during PAH development. Mice with SMC-specific FLNA deficiency were protected from hypoxia-induced pulmonary hypertension and pulmonary vascular remodeling. Furthermore, PAK1 may act as a downstream signaling target of FLNA. Collectively, these data suggested that FLNA and associated pathways could be a viable target for the treatment of PAH in clinical settings.

Availability of data and materials

The datasets used and/or analyzed during the current study are available from the corresponding author on reasonable request.

Authors' contributions

All authors participated in the design and interpretation of the study, the analysis of the data and the review of the manuscript. YGZ, SL and SLC designed the study, interpreted the data and revised the manuscript critically. HM and PY conducted the majority of the experiments, performed the statistical analysis and wrote the manuscript. YFY and WDY conducted parts of the experiments. All authors read and approved the final manuscript. SL and SLC confirm the authenticity of all the raw data.

Ethics approval and consent to participate

For experiments involving human tissues, approval was obtained from the Ethics Committees of Nanjing Medical University (approval no. KY20190505-09), and all subjects gave informed consent before the study. The animal study was reviewed and approved by the Institutional Animal Care and Use Committee of Nanjing Medical University, and conformed with the guide for the care and use of laboratory animals (approval no. 1905004). Ethics approval for the use of HPASMCs was obtained from the Ethics Committees of the Nanjing Medical University.

Patient consent for publication

Not applicable.

Competing interests

The authors declare that they have no competing interests.

References

1. Vazquez ZGS and Klinger JR: Guidelines for the treatment of pulmonary arterial hypertension. Lung 198: 581-596, 2020.
2. Christou H and Khalil RA: Mechanisms of pulmonary vascular dysfunction in pulmonary hypertension and implications for novel therapies. Am J Physiol Heart Circ Physiol 322: H702-H704, 2022.
3. Zhang L, Wang Y, Wu G, Rao L, Wei Y, Yue H, Yuan T, Yang P, Xiong F, Zhang S, *et al*: Blockade of JAK2 protects mice against hypoxia-induced pulmonary arterial hypertension by repressing pulmonary arterial smooth muscle cell proliferation. Cell Prolif 53: e12742, 2020.
4. Zheng YG, Ma H, Chen L, Jiang XM, Zhou L, Lin S and Chen SL: Efficacy and safety of oral targeted therapies in pulmonary arterial hypertension: A meta-analysis of randomized clinical trials. Pulm Circ 8: 2045894018798183, 2018.
5. Zhou J, Kang X, An H, Lv Y and Liu X: The function and pathogenic mechanism of filamin A. Gene 784: 145575, 2021.
6. Bandaru S, Ala C, Zhou AX and Akyürek LM: Filamin A regulates cardiovascular remodeling. Int J Mol Sci 22: 6555, 2021.
7. Eltahir S, Ahmad KS, Al-Balawi MM, Bukhamsien H, Al-Mobaireek K, Alotaibi W and Al-Shamrani A: Lung disease associated with filamin A gene mutation: A case report. J Med Case Rep 10: 97, 2016.
8. Burrage LC, Guillerman RP, Das S, Singh S, Schady DA, Morris SA, Walkiewicz M, Schecter MG, Heinle JS, Lotze TE, *et al*: Lung transplantation for FLNA-associated progressive lung disease. J Pediatr 186: 118-123.e6, 2017.
9. Hirashiki A, Adachi S, Nakano Y, Kamimura Y, Ogo T, Nakanishi N, Morisaki T, Morisaki H, Shimizu A, Toba K, *et al*: Left main coronary artery compression by a dilated main pulmonary artery and left coronary sinus of Valsalva aneurysm in a patient with heritable pulmonary arterial hypertension and FLNA mutation. Pulm Circ 7: 734-740, 2017.
10. Stossel TP, Condeelis J, Cooley L, Hartwig JH, Noegel A, Schleicher M and Shapiro SS: Filamins as integrators of cell mechanics and signalling. Nat Rev Mol Cell Biol 2: 138-145, 2001.
11. Retailleau K, Arhatte M, Demolombe S, Peyronnet R, Baudrie V, Jodar M, Bourreau J, Henrion D, Offermanns S, Nakamura F, *et al*: Arterial myogenic activation through smooth muscle filamin A. Cell Rep 14: 2050-2058, 2016.
12. Huang L, Li L, Hu E, Chen G, Meng X, Xiong C and He J: Potential biomarkers and targets in reversibility of pulmonary arterial hypertension secondary to congenital heart disease: An explorative study. Pulm Circ 8: 2045893218755987, 2018.
13. National Research Council (NRC): Institute for Laboratory Animal Research: Guide for the care and use of laboratory animals. 8th edition. National Academies Press, Washington, DC, 2011.
14. Gomez-Arroyo J, Saleem SJ, Mizuno S, Syed AA, Bogaard HJ, Abbate A, Taraseviciene-Stewart L, Sung Y, Kraskauskas D, Farkas D, *et al*: A brief overview of mouse models of pulmonary arterial hypertension: problems and prospects. Am J Physiol Lung Cell Mol Physiol 302: L977-L991, 2012.
15. Ciuclan L, Bonneau O, Hussey M, Duggan N, Holmes AM, Good R, Stringer R, Jones P, Morrell NW, Jarai G, *et al*: A novel murine model of severe pulmonary arterial hypertension. Am J Respir Crit Care Med 184: 1171-1182, 2011.
16. Vitali SH, Hansmann G, Rose C, Fernandez-Gonzalez A, Scheid A, Mitsialis SA and Kourembanas S: The Sugen 5416/hypoxia mouse model of pulmonary hypertension revisited: Long-term follow-up. Pulm Circ 4: 619-629, 2014.
17. Liu PF, Zhang AK, Ding Z, Dai D, Li B, Liu SF, Xu J, Cheng Z, Zhao S, Zhao X and Dong J: m^{6}A modification-mediated GRAP regulates vascular remodeling in hypoxic pulmonary hypertension. Am J Respir Cell Mol Biol 67: 574-588, 2022.
18. Woo MS, Ohta Y, Rabinovitz I, Stossel TP and Blenis J: Ribosomal S6 kinase (RSK) regulates phosphorylation of filamin A on an important regulatory site. Mol Cell Biol 24: 3025-3035, 2004.
19. Huang L, Li L, Yang T, Li W, Song L, Meng X, Gu Q, Xiong C and He J: Transgelin as a potential target in the reversibility of pulmonary arterial hypertension secondary to congenital heart disease. J Cell Mol Med 22: 6249-6261, 2018.
20. Livak KJ and Schmittgen TD: Analysis of relative gene expression data using real-time quantitative PCR and the 2(-Delta Delta C(T)) method. Methods 25: 402-408, 2001.
21. Casique-Aguirre D, Briseño-Díaz P, García-Gutiérrez P, la Rosa CHG, Quintero-Barceinas RS, Rojo-Domínguez A, Vergara I, Medina LA, Correa-Basurto J, Bello M, *et al*: KRas4B-PDE6δ complex stabilization by small molecules obtained by virtual screening affects Ras signaling in pancreatic cancer. BMC Cancer 18: 1299, 2018.
22. Feng Y, Chen MH, Moskowitz IP, Mendonza AM, Vidali L, Nakamura F, Kwiatkowski DJ and Walsh CA: Filamin A (FLNA) is required for cell-cell contact in vascular development and cardiac morphogenesis. Proc Natl Acad Sci USA 103: 19836-19841, 2006.
23. Deng X, Li S, Qiu Q, Jin B, Yan M, Hu Y, Wu Y, Zhou H, Zhang G and Zheng X: Where the congenital heart disease meets the pulmonary arterial hypertension, FLNA matters: A case report and literature review. BMC Pediatr 20: 504, 2020.
24. Demirel N, Ochoa R, Dishop MK, Holm T, Gershan W and Brottman G: Respiratory distress in a 2-month-old infant: Is the primary cause cardiac, pulmonary or both? Respir Med Case Rep 25: 61-65, 2018.
25. Masurel-Paulet A, Haan E, Thompson EM, Goizet C, Thauvin-Robinet C, Tai A, Kennedy D, Smith G, Khong TY, Solé G, *et al*: Lung disease associated with periventricular nodular heterotopia and an FLNA mutation. Eur J Med Genet 54: 25-28, 2011.
26. Sasaki E, Byrne AT, Phelan E, Cox DW and Reardon W: A review of filamin A mutations and associated interstitial lung disease. Eur J Pediatr 178: 121-129, 2019.
27. Zheng X, Zhou AX, Rouhi P, Uramoto H, Borén J, Cao Y, Pereira T, Akyürek LM and Poellinger L: Hypoxia-induced and calpain-dependent cleavage of filamin A regulates the hypoxic response. Proc Natl Acad Sci USA 111: 2560-2565, 2014.
28. Wang K, Ash JF and Singer SJ: Filamin, a new high-molecular-weight protein found in smooth muscle and non-muscle cells. Proc Natl Acad Sci USA 72: 4483-4486, 1975.
29. Jain M, Weber A, Maly K, Manjaly G, Deek J, Tsvyetkova O, Stulić M, Toca-Herrera JL and Jantsch MF: A-to-I RNA editing of filamin A regulates cellular adhesion, migration and mechanical properties. FEBS J 289: 4580-4601, 2022.

30. Karimi A and Milewicz DM: Structure of the elastin-contractile units in the thoracic aorta and how genes that cause thoracic aortic aneurysms and dissections disrupt this structure. Can J Cardiol 32: 26-34, 2016.

31. Yu N, Erb L, Shivaji R, Weisman GA and Seye CI: Binding of the P2Y2 nucleotide receptor to filamin A regulates migration of vascular smooth muscle cells. Circ Res 102: 581-588, 2008.

32. Pena E, Arderiu G and Badimon L: Subcellular localization of tissue factor and human coronary artery smooth muscle cell migration. J Thromb Haemost 10: 2373-2382, 2012.

33. Retailleau K, Arhatte M, Demolombe S, Jodar M, Baudrie V, Offermanns S, Feng Y, Patel A, Honoré E and Duprat F: Smooth muscle filamin A is a major determinant of conduit artery structure and function at the adult stage. Pflugers Arch 468: 1151-1160, 2016.

34. Chen Y, Wei X, Zhang ZH, He Y, Huo B, Guo X, Feng X, Fang ZM, Jiang DS and Zhu XH: Downregulation of filamin A expression in the aorta is correlated with aortic dissection. Front Cardiovasc Med 8: 690846, 2021.

35. Maceyka M, Alvarez SE, Milstien S and Spiegel S: Filamin A links sphingosine kinase 1 and sphingosine-1-phosphate receptor 1 at lamellipodia to orchestrate cell migration. Mol Cell Biol 28: 5687-5697, 2008.

36. Vadlamudi RK, Li F, Adam L, Nguyen D, Ohta Y, Stossel TP and Kumar R: Filamin is essential in actin cytoskeletal assembly mediated by p21-activated kinase 1. Nat Cell Biol 4: 681-690, 2002.

37. Shimokawa H, Sunamura S and Satoh K: RhoA/Rho-kinase in the cardiovascular system. Circ Res 118: 352-366, 2016.

38. Dilasser F, Rio M, Rose L, Tesse A, Guignabert C, Loirand G and Sauzeau V: Smooth muscle Rac1 contributes to pulmonary hypertension. Br J Pharmacol 179: 3418-3429, 2022.

39. Johnson JA, Hemnes AR, Perrien DS, Schuster M, Robinson LJ, Gladson S, Loibner H, Bai S, Blackwell TR, Tada Y, et al: Cytoskeletal defects in Bmpr2-associated pulmonary arterial hypertension. Am J Physiol Lung Cell Mol Physiol 302: L474-L484, 2012.

40. Kim HJ, Ryu KJ, Kim MJ, Kim T, Kim SH, Han H, Kim H, Hong KS, Song Y, Choi Y, et al: RhoGDI2-mediated rac1 recruitment to filamin A enhances Rac1 activity and promotes invasive abilities of gastric cancer cells. Cancers (Basel) 14: 255, 2022.

41. Hinoki A, Kimura K, Higuchi S, Eguchi K, Takaguri A, Ishimaru K, Frank GD, Gerthoffer WT, Sommerville LJ, Autieri MV and Eguchi S: p21-activated kinase 1 participates in vascular remodeling in vitro and in vivo. Hypertension 55: 161-165, 2010.

42. Wang D, Paria BC, Zhang Q, Karpurapu M, Li Q, Gerthoffer WT, Nakaoka Y and Rao GN: A role for Gab1/SHP2 in thrombin activation of PAK1: Gene transfer of kinase-dead PAK1 inhibits injury-induced restenosis. Circ Res 104: 1066-1075, 2009.

43. Fediuk J, Sikarwar AS, Nolette N and Dakshinamurti S: Thromboxane-induced actin polymerization in hypoxic neonatal pulmonary arterial myocytes involves Cdc42 signaling. Am J Physiol Lung Cell Mol Physiol 307: L877-L887, 2014.

44. Diebold I, Petry A, Djordjevic T, Belaiba RS, Fineman J, Black S, Schreiber C, Fratz S, Hess J, Kietzmann T and Görlach A: Reciprocal regulation of Rac1 and PAK-1 by HIF-1alpha: A positive-feedback loop promoting pulmonary vascular remodeling. Antioxid Redox Signal 13: 399-412, 2010.